



OPEN

Optical investigation of the natural electron doping in thin MoS₂ films deposited on dielectric substrates

SUBJECT AREAS:

ELECTRONIC DEVICES

TWO-DIMENSIONAL MATERIALS

SURFACES, INTERFACES AND THIN FILMS

PHOTONIC DEVICES

D. Sercombe¹, S. Schwarz¹, O. Del Pozo-Zamudio¹, F. Liu^{1,2}, B. J. Robinson³, E. A. Chekhovich¹, I. I. Tartakovskii⁴, O. Kolosov³ & A. I. Tartakovskii¹¹Department of Physics and Astronomy, University of Sheffield, Sheffield S3 7RH, United Kingdom, ²Experimentelle Physik 2, Technische Universität Dortmund, 44221 Dortmund, Germany, ³Department of Physics, University of Lancaster, Lancaster LA1 4YB, United Kingdom, ⁴Institute of Solid State Physics, Russian Academy of Sciences, Chernogolovka, 142432, Russia.Received
12 June 2013Accepted
27 November 2013Published
12 December 2013

Correspondence and requests for materials should be addressed to A.I.T. (a.tartakovskii@sheffield.ac.uk)

Two-dimensional (2D) compounds provide unique building blocks for novel layered devices and hybrid photonic structures. However, large surface-to-volume ratio in thin films enhances the significance of surface interactions and charging effects requiring new understanding. Here we use micro-photoluminescence (PL) and ultrasonic force microscopy to explore the influence of the dielectric environment on optical properties of a few monolayer MoS₂ films. PL spectra for MoS₂ films deposited on SiO₂ substrates are found to vary widely. This film-to-film variation is suppressed by additional capping of MoS₂ with SiO₂ and Si_xN_y, improving mechanical coupling of MoS₂ with surrounding dielectrics. We show that the observed PL non-uniformities are related to strong variation in the local electron charging of MoS₂ films. In completely encapsulated films, negative charging is enhanced leading to uniform optical properties. Observed great sensitivity of optical characteristics of 2D films to surface interactions has important implications for optoelectronics applications of layered materials.

Interest in atomically thin two-dimensional (2D) layered compounds is growing due to unique physical properties found for monolayer (ML) structures^{1,2}. One such material, molybdenum disulfide (MoS₂), has generated particular interest due to the presence of an indirect-to-direct band gap transition and observation of photoluminescence (PL)^{3–5} and electro-luminescence⁶ in the visible range up to room temperature. A high on/off ratio (exceeding 10⁸) has suggested a potential use in field effect transistors⁷, while a strong valley polarization is likely to be used in the development of future valleytronics applications^{8–12}.

PL studies⁴ have shown that suspended ML films of MoS₂ have enhanced emission compared to those in contact with the substrate. However, the eventual integration of MoS₂ into devices, such as transistors and photonic structures, will render the use of suspended MoS₂ impractical. The effect of dielectric encapsulation has so far been reported for high-*k* dielectric materials commonly used in transistors^{13–15}. However, no thorough study showing how dielectric environments affect optical properties and charging of MoS₂ films has yet been conducted, the two issues we address in this work.

We focus on interaction of MoS₂ films with SiO₂ and Si_xN_y, commonly used in photonic devices, and report low temperature PL measurements on over a 100 thin films, enabling detailed insight in interactions of MoS₂ with its dielectric surrounding. We study mechanically exfoliated MoS₂ films deposited on silicon substrates finished with either nearly atomically flat thermally grown SiO₂ or relatively rough SiO₂ grown by plasma-enhanced chemical vapor deposition (PECVD). We use a combination of low temperature micro-photoluminescence (PL), atomic force microscopy (AFM) and ultrasonic force microscopy (UFM). We find marked variety of the PL spectral lineshapes and peak energies in the large number of few monolayer MoS₂ films, which nonetheless show trends that we are able to relate to electrostatic and mechanical interaction of thin films with the surrounding dielectrics.

We find that high mechanical coupling between a MoS₂ film and the surrounding layers is only possible for capped films on thermally grown SiO₂, whereas more complex morphology and poorer contact with the surrounding layers is observed for uncapped films, the effect further exacerbated for films on higher roughness PECVD substrates. Following this observation, we show a direct correlation between the enhanced mechanical coupling of MoS₂ with the surrounding dielectric layers and increased negative charging of the films, directly affecting spectral characteristics of PL due to the presence of the pronounced PL peak of a negatively charged



trion. By comparison with recent work where MoS₂ films were controllably charged by applying voltage¹⁶, we estimate that observed charging lead to electron densities of the order of 10¹² cm⁻².

Results

PL of thin MoS₂ films. We carry out low-temperature PL spectroscopy on a wide range of MoS₂ films having thicknesses between 2 and 5 ML, as estimated from the careful colour-contrast examination using optical microscopy, and further confirmed for some films from AFM measurement (see Methods for description of sample fabrication and PL techniques). Fig. 1(a) shows a selection of PL spectra measured for uncapped MoS₂ films deposited on Si substrates with either PECVD (a–d) or thermal oxidation (e–h). In all spectra exciton complexes *A* and *B* are clearly visible³, although there is a large variation in PL lineshapes for different films. The *A* complex is composed of a trion PL peak *A*⁻ and a high energy shoulder *A*⁰ corresponding to neutral exciton PL¹⁶. A low energy shoulder *L* is also observed in some spectra, though spectra showing weak or no contributions of *L* and *A*⁰ states were observed on both PECVD (a) and thermal oxide (e) substrates. A relatively large contribution of *L* and *A*⁰ was found in many films deposited on PECVD substrates (b, c) and in some cases the neutral exciton was found to have brighter emission than the trion [as in (d)]. For films deposited on thermal oxide substrates, there is a less significant variation in the lineshape (e–h), and *L* and *A*⁰ features are, in general, less pronounced relative to *A*⁻ than in films deposited on PECVD grown SiO₂.

The effect of additional capping of MoS₂ films with dielectric layers is demonstrated in Fig. 2. A 100 nm thick layer of either SiO₂ or Si_xN_y is deposited using PECVD on top of the MoS₂/SiO₂/Si samples for both PECVD and thermal SiO₂/Si substrates. Here we observe even less variation in lineshapes between the films. A further suppression of the low energy shoulder *L* and neutral exciton peak *A*⁰ is found for films capped with Si_xN_y (a,b,e,f) on both types of substrates, and with SiO₂ on thermally grown substrates. In contrast, *L* and *A*⁰ peaks are pronounced when capping with SiO₂ is used for MoS₂ films on PECVD substrates. Further to this, from comparison of spectra in (a,b,c,d) and (e,f,g,h), we find that the PL linewidths of

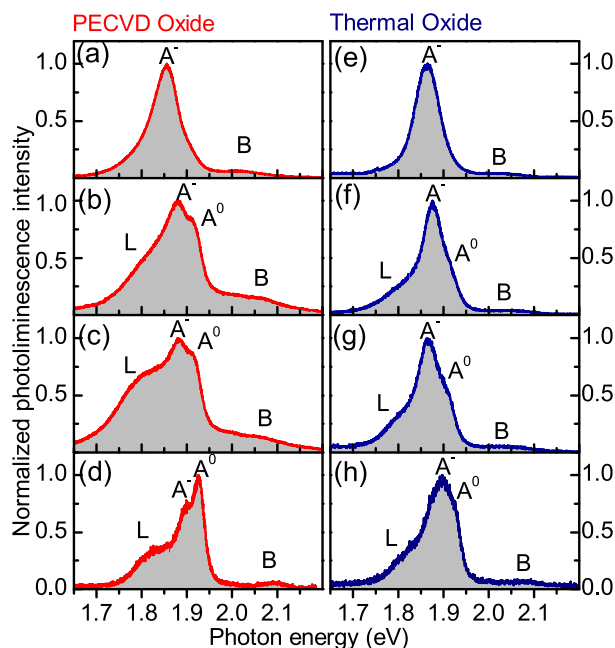


Figure 1 | PL spectra measured for individual mechanically exfoliated MoS₂ uncapped films deposited on a 300 nm SiO₂ layer grown by either PECVD (a–d) or thermal oxidation (e–h) on a silicon substrate.

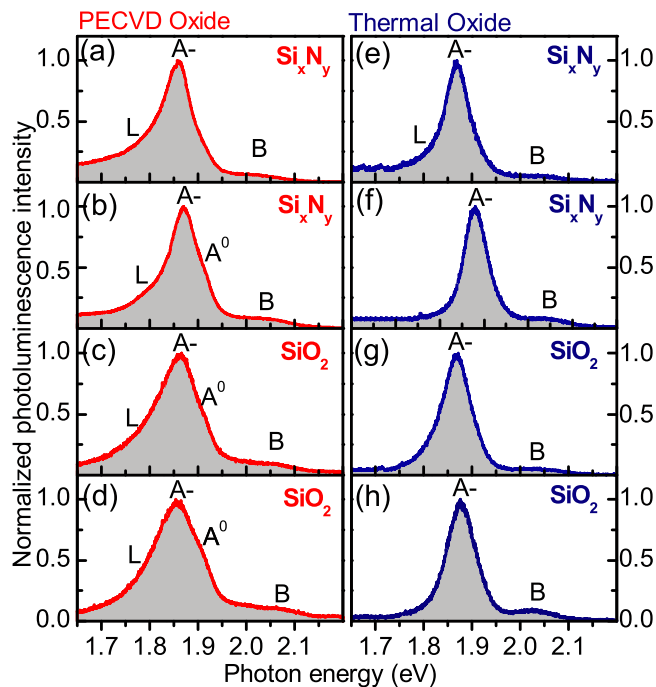


Figure 2 | PL spectra measured for individual mechanically exfoliated MoS₂ films capped by a 100 nm PECVD layer of dielectric material. The effect of capping is shown for films deposited on PECVD grown SiO₂ substrates for Si_xN_y (a), (b) and SiO₂ (c), (d) capping layers, and also for films deposited on thermally grown SiO₂ and capped with Si_xN_y (e), (f) and SiO₂ (g), (h).

films deposited on the PECVD oxide are notably broader than for those on the thermal oxide substrates.

An interesting trend in all spectra presented in Figs. 1 and 2 is a correlation between the intensities of the features *L* and *A*⁰: the two peaks are either both rather pronounced or suppressed in any given spectrum relative to the trion peak *A*⁻. This may imply that peak *L* becomes suppressed when the film captures an excess of negative charge.

Analysis of PL peak energies. A statistical analysis of PL peak energies for films deposited on the two types of substrates is presented in Fig. 3. Fig. 3(a,b) show that the average values for the PL peak energies, E_{max}^{av} , for uncapped films are $E_{max}^{av} = 1.888$ eV for the PECVD substrates and $E_{max}^{av} = 1.880$ eV for thermal oxide substrates, with an almost two times larger standard deviation, σ_{Emax} for the former (18 versus 11 meV). The data collected for the capped films (shaded for Si_xN_y and hatched for SiO₂) are presented in Fig. 3(c) and (d) for the thermal and PECVD oxide substrates, respectively. Significant narrowing of the peak energy distribution is found in all cases: $\sigma_{Emax} \approx 6$ meV has been found. The average peak energies are very similar for both SiO₂ and Si_xN_y capping on the thermal oxide substrates ($E_{max}^{av} = 1.874$ eV), but differ for PECVD substrates: $E_{max}^{av} = 1.862$ and 1.870 eV for SiO₂ and Si_xN_y capping, respectively.

From previous reports⁴, for films with thicknesses in the range 2 to 5 MLs, one can expect the PL peak shift on the order of 20 meV. In addition, PL yield was reported to be about 10 times higher for 2 ML films compared with 4 ML and for 3 ML compared with 5 ML⁴. In our study, the integrated PL signal shows a large variation within about one order of magnitude between the films. The dependence of the PL yield on the type of the substrate and capping is not very pronounced. While our data for PL intensities is consistent with the reported in the literature for the range of thicknesses which we studied, the PL peak energy distribution shows the unexpected

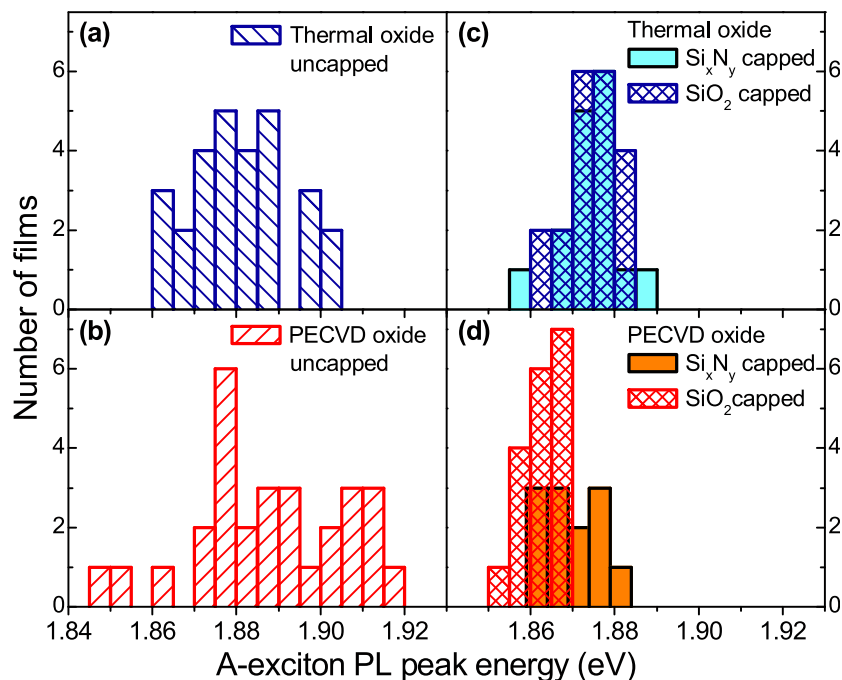


Figure 3 | (a–d) PL peak energies for *A* exciton complex in MoS₂ thin films. Data for films deposited on thermally (PECVD) grown SiO₂ substrates are shown in top (bottom) panels. Panels (a)–(b) and (c)–(d) show PL peak positions for uncapped and capped films, respectively.

broadening for uncapped samples: for example, deviations from E_{max}^{av} by ± 20 –30 meV are evident in Fig. 3(a,b). For the capped samples, new trends are observed: the significant narrowing and red-shift of E_{max} distributions. As shown below, these effects reflect changes in the PL lineshapes between the capped and uncapped samples, which in their turn reflect changes in the relative intensities of the A^- , A^0 and L peaks.

We note that the new experimental trends observed in our PL studies do not depend on the exact distribution of thicknesses in the ensembles of the investigated films, provided these distributions

are similar for all types of samples studied. The latter is the case in our study, as the films were produced using the same method, show similar range of the colour-contrasts under optical examination, and exhibit similar ranges of PL yield.

Analysis of PL lineshapes. In this section we will present the line-shape analysis for the *A* exciton PL based on the measurement of full width at half maximum (FWHM) in each PL spectrum. This approach allows one to account for contributions of the three PL features, L , A^0 and A^- . The data are summarized in Fig. 4 and Table 1.

PECVD grown SiO₂ substrates. These data are presented in Fig. 4 in red. Data for uncapped films are shown in Fig. 4(a), from where it is evident that the lineshapes vary dramatically from film to film within a range from 50 to 170 meV. FWHM for uncapped films on PECVD grown substrates is on average $\Delta E_{FWHM}^{av} = 96$ with a large standard deviation $\sigma_{FWHM} = 33$ meV. This gives a rather high coefficient of variation $\sigma_{FWHM} / \Delta E_{FWHM}^{av} = 0.34$.

The non-uniformity of lineshapes of the PL spectra is significantly suppressed by capping the films with Si_xN_y and SiO₂ (shown with red in Fig. 4(b) and (c), respectively). This is evidenced from the reduction of the coefficient of variation in the FWHM values by a factor of 4 in capped films compared with the uncapped samples (in Table 1). Despite the narrowed spread of ΔE_{FWHM} values, the average FWHM

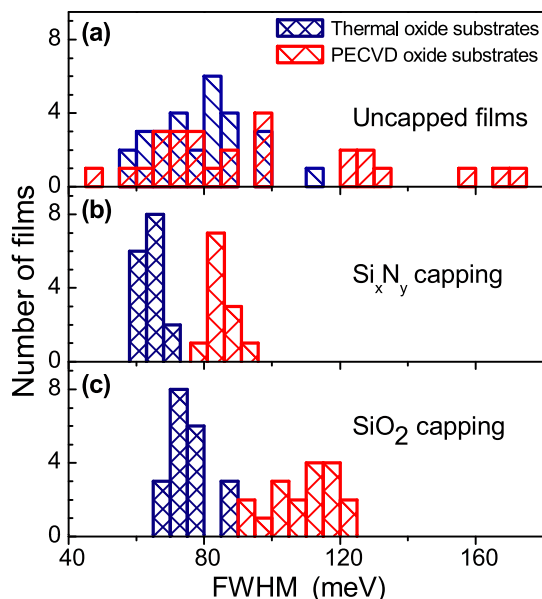


Figure 4 | PL FWHM of exciton complex *A* in thin MoS₂ films. Data for MoS₂ films deposited on thermally and PECVD grown SiO₂ substrates is shown with blue and red, respectively. (a) PL FWHM of uncapped MoS₂ films. (b) PL FWHM of Si_xN_y capped MoS₂ films. (c) PL FWHM of SiO₂ capped MoS₂ films.

Table 1 | Mean values, standard deviations and coefficients of variation for full width at half maximum of PL spectra measured for thin MoS₂ films

Substrate/Capping	Mean value	Standard deviation	Coefficient of variation
PECVD/uncapped	96 meV	33 meV	0.34
PECVD/SiO ₂	109 meV	9 meV	0.08
PECVD/Si _x N _y	84 meV	7 meV	0.08
Thermal/uncapped	79 meV	12 meV	0.15
Thermal/SiO ₂	76 meV	7 meV	0.09
Thermal/Si _x N _y	64 meV	4 meV	0.06



in SiO₂ capped films is rather high, 109 meV, which reflects relatively strong contribution of *L* and A⁰ PL features. Contributions of A⁻, *L* and A⁰ features vary very considerably in the uncapped samples, leading to on average smaller linewidths but a very significant spread in FWHM values. In contrast, in Si_xN_y capped films, A⁻ peak dominates and both *L* and A⁰ features are relatively weak, which effectively results in narrowing of PL.

Thermally grown SiO₂ substrates. These data are presented in Fig. 4 in blue. It can be seen that uncapped films deposited on the flatter thermal oxide substrates appear to have significantly narrower distributions of linewidths compared to uncapped films on PECVD substrates: coefficient of variation of ΔE_{FWHM} is by a factor of 2 smaller for films on the thermally grown substrates [see Fig. 4(a) and Table 1]. In addition, compared with the films deposited on PECVD grown SiO₂, FWHM is also reduced by about 20% to 79 meV. Such narrowing reflects weaker contribution of *L* and A⁰ peaks in PL spectra.

The non-uniformity of the PL spectra still present in uncapped films deposited on thermally grown SiO₂ is further suppressed by capping the films with Si_xN_y and SiO₂ [shown with blue in Fig. 4(b) and (c), respectively]. In general, the coefficients of variation for FWHM of the capped films are rather similar for both substrates and are in the range of 0.06–0.09, showing significant improvement of the reproducibility of PL features showing compared with the uncapped samples (see Table 1). For Si_xN_y capped films on thermally grown SiO₂, we also observe narrowing of PL emission to $\Delta E_{FWHM}^{av} = 64$ meV. This reflects further suppression of *L* and A⁰ peaks relative to A⁻, the effect less pronounced in SiO₂ capped films.

AFM and UFM measurements. To further understand the interactions between MoS₂ films and the substrate/capping materials, we carried out detailed AFM and UFM measurements of our samples (Fig. 5). AFM measurements of films deposited on PECVD grown substrates Fig. 5(a) show that the film is distorted in shape and follows the morphology of the underlying substrate. The root mean square (rms) roughness R_{rms} of these films is 1.7 nm with a maximum height $R_{max} = 11$ nm, similar to the parameters of the substrate, $R_{rms} = 2$ nm and $R_{max} = 15$ nm. Such R_{max} is greater than the thickness of films (<3 nm), leading to significant film distortions. UFM measurements of these films [Fig. 5(b)] show small areas of higher stiffness (light colour, marked with arrows) and much larger areas of low stiffness (i.e. no contact with the substrate) shown with a dark colour. This shows that the film is largely suspended above the substrate on point contacts.

AFM measurements of films deposited on thermally grown SiO₂ substrates [Fig. 5(c)] show a much more uniform film surface due to the less rough underlying substrate. This is reflected in a significantly improved $R_{rms} = 0.3$ nm and $R_{max} = 1.8$ nm. These values are still higher than those for the bare substrate with $R_{rms} = 0.09$ nm and $R_{max} = 0.68$ nm. A more uniform stiffness distribution is observed for these films in UFM [Fig. 5(d)], although the darker colour of the film demonstrates that it is much softer than the surrounding substrate and thus still has relatively poor contact with the substrate. A darker shading at film edges demonstrates that they have poorer contact than the film center and effectively curl away from the substrate.

AFM and UFM data for films capped with 15 nm SiO₂ after deposition on PECVD and thermally grown SiO₂ are given in Fig. 5(e, f) and (g, h), respectively. For the PECVD substrate, the roughness of the MoS₂ film is similar to that in the uncapped sample in Fig. 5(a): $R_{rms} = 1.68$ nm and $R_{max} = 10.2$ nm. From the UFM data in Fig. 5(f), it is evident that although the contact of the MoS₂ film with the surrounding SiO₂ is greatly improved compared with the uncapped films, a large degree of non-uniformity is still present, as concluded from many dark spots on the UFM image. In great contrast to that, the capped MoS₂ film on thermally grown SiO₂ is

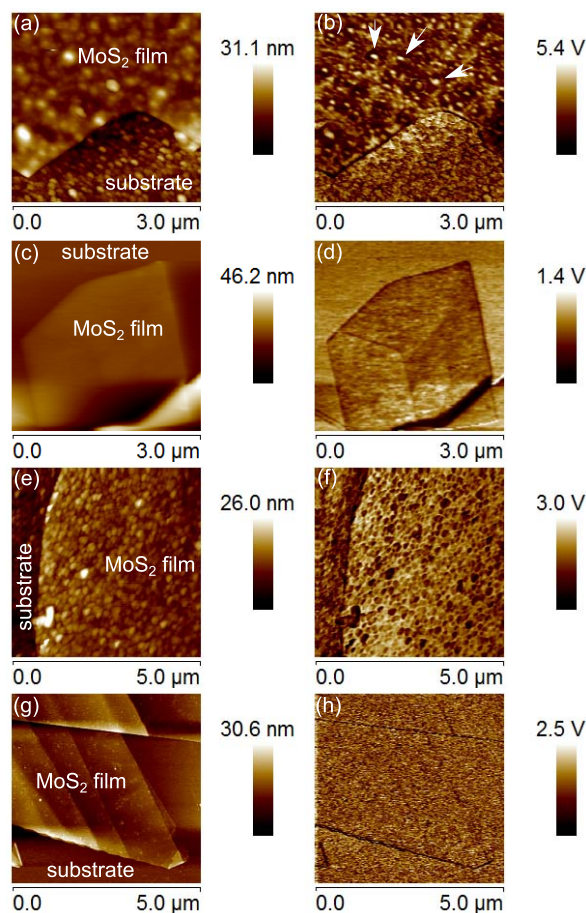


Figure 5 | AFM (left column) and UFM (right column) images for MoS₂ thin films deposited on PECVD and thermally grown SiO₂ substrates. (a), (b) PECVD substrate, uncapped MoS₂ film; (c), (d) thermally grown substrate, uncapped MoS₂ film; (e), (f) PECVD substrate, MoS₂ film capped with 15 nm of SiO₂ grown by PECVD; (g), (h) thermally grown substrate, MoS₂ film capped with 15 nm of SiO₂ grown by PECVD.

flatter [Fig. 5(g, h)], $R_{rms} = 0.42$ nm and $R_{max} = 6.1$ nm, with the roughness most likely originating from the PECVD grown SiO₂ capping layer. The UFM image in Fig. 5(h) shows remarkable uniformity of the stiffness of the film similar to that of the capped substrate, demonstrating uniform and firm contact (i.e. improved mechanical coupling) between the MoS₂ film and the surrounding dielectrics.

Discussion

There is a marked correlation between the PL properties of the MoS₂ films and film stiffness measured by UFM. The stiffness reflects the strength of the mechanical coupling between the adjacent monolayers of the MoS₂ film and the surrounding dielectrics. The increased bonding and its uniformity for films deposited on less rough thermally grown SiO₂ substrates and for capped MoS₂ films manifests in the more reproducible PL characteristics, leading to reduced standard deviations of the peak positions and linewidths. These spectral characteristics are influenced by the relative intensities of the three dominating PL features, trion A⁻, neutral exciton A⁰ and low energy *L* peak, which are influenced by the charge balance in the MoS₂ films sensitive to the dielectric environment. The efficiency of charging can be qualitatively estimated from the relative intensities of A⁻ and A⁰ peaks. In the vast majority of the films, A⁻ dominates. As noted above, the intensity of A⁰ directly correlates (qualitatively) with that of the relatively broad low energy PL shoulder *L* (see Fig. 1 and 2), previously ascribed to emission from surface states. The line-



shape analysis presented in Fig. 4 and Table 1 is particularly sensitive to the contribution of peak L .

The PL lineshape analysis and comparison with the UFM data lead to conclusion that negative charging of the MoS₂ films is relatively inefficient for partly suspended uncapped films on rough PECVD substrates. Both in SiO₂ and Si_xN_y capped films on PECVD substrates, the charging effects are more pronounced. However, both A^0 and L features still have rather high intensities. The relatively low charging efficiency is most likely related to a non-uniform bonding between the MoS₂ films and the surrounding dielectric layers as concluded from UFM data [see Fig. 5(f)]. The charging is more pronounced for uncapped MoS₂ films on thermal oxide substrates, and is enhanced significantly more for capped films: for Si_xN_y capping A^0 and L peaks only appear as weak shoulders in PL spectra.

It is clear from this analysis that the charge balance in the MoS₂ films is altered strongly when the films are brought in close and uniform contact with the surrounding dielectrics, enabling efficient transfer of charge in a monolithic hybrid heterostructure. Both n -type^{4,7,17} and p -type^{17,18} conductivities have been reported in thin MoS₂ films deposited on SiO₂. It is thus possible that the sign and density of charges in exfoliated MoS₂ films may be strongly affected by the properties of PECVD grown SiO₂ and Si_xN_y, where the electronic properties may vary depending on the growth conditions^{19–21}. It is notable, however, that for a large variety of samples studied in this work, the negative charge accumulation in the MoS₂ films is pronounced, and is further enhanced when the bonding of the films with the dielectric layers is improved.

In order to estimate the density of the accumulated charges we refer to Ref. 16, where PL spectra as a function of electron density in the film were measured. The neutral exciton PL peak A^0 becomes less intense than the trion peak A^- at the electron density $n \approx 2 \times 10^{12} \text{ cm}^{-2}$. Since in our experiments in many films A^0 peak is relatively pronounced, we conclude that we have studied the regime where the electron densities are of the order of 10^{12} cm^{-2} or less.

The band-structure of MoS₂ and hence its optical characteristics can also be influenced by strain^{22–24}. However, the distribution and magnitude of strain cannot be assessed directly in our experiments. Indirect evidence for increased tensile strain in capped samples compared to uncapped films on PECVD may be deduced from the red-shift of the average PL peak energy by ~ 20 meV after capping (data in Fig. 3). On the other hand, doping-dependent Stokes shifts of the trion PL have been found recently¹⁶, which may explain the behavior we find in charged MoS₂ sheets. One would expect a more uniform strain distribution in the case of uniform mechanical properties of the sample, which as shown by UFM is achieved for capped MoS₂ films on flat thermally grown SiO₂ substrates. In order to roughly estimate a possible magnitude of strain in our films we refer to recent work in Refs. 24–26 reporting 50 to 80 meV bandgap shift per percent of applied strain. This implies that in our experiments the maximum strain in the films reaches $\approx 0.5\%$.

We note, that another method for sensing the strain and charging in thin MoS₂ films is by using Raman spectroscopy. Recently it has been found that Raman modes²⁷ E_{2g}^1 and A_{1g} exhibit frequency shifts under the influence of strain^{25,26,28} and charging²⁹. We have also carried out preliminary Raman experiments on a set of films placed on PECVD and thermally grown SiO₂ substrates and capped with SiO₂ and Si_xN_y. However, only very weak trends have been observed. This is consistent with relatively low charging densities and strain in our samples, the effect of which is readily detectable in PL^{16,25,26}, but is less pronounced in Raman measurements.

In conclusion, we demonstrate that it is possible to increase the reproducibility of optical characteristics of mechanically exfoliated few mono-layer MoS₂ films by coating the films with additional dielectric layers of either SiO₂ or Si_xN_y. By comparing PL data with results obtained in UFM, we show that there is a direct correlation between the degree of the mechanical coupling of the MoS₂ films to

the surrounding dielectrics and uniformity of the optical properties. We show that a wide spread in PL spectral lineshapes occurs in general as a result of the film-to-film variation of the relative intensities of the negatively charged trion peak A^- and the two other features, neutral exciton peak A^0 and a low energy PL band L . We find that when the mechanical coupling between the films and the dielectrics is improved, the films become increasingly negatively charged, as deduced from the pronounced increase in PL of the trion peak, dominating in the majority of PL spectra. Such charging, and also possibly reduction in strain non-uniformities, underpins the highly uniform PL properties in capped MoS₂ films, leading to the smallest linewidths below 70 meV for thin MoS₂ films deposited on thermally grown SiO₂ and capped with a Si_xN_y layer.

Note: Since this work has been submitted, two more detailed studies of interaction of MoS₂ films with substrates have become available^{30,31}.

Methods

Sample preparation. MoS₂ was exfoliated using the mechanical cleavage method¹ and deposited on commercially purchased Si wafers with a low roughness 300 nm thick thermally grown SiO₂³². Further MoS₂ samples were produced using the same technique, but deposited on Si substrates covered with 300 nm PECVD grown SiO₂. PECVD deposition was done in a 60°C chamber with a sample temperature of 300°C. The root mean square (rms) roughness, R_{rms} , of the PECVD grown SiO₂ is found to be 2 nm with a maximum peak height of 15 nm, whereas R_{rms} of the thermally grown SiO₂ is 0.09 nm with a maximum height of 0.68 nm. The additional capping of the MoS₂/SiO₂/Si samples with Si_xN_y and SiO₂ was carried out using the same PECVD techniques. The complete SiO₂/MoS₂/SiO₂/Si or Si_xN_y/MoS₂/SiO₂/Si samples had the top Si_xN_y and SiO₂ layers with thicknesses of 100 nm for PL and 15 nm for AFM/UFM measurements. The high surface roughness rendered impractical use of AFM for measurements of the film thicknesses on PECVD substrates. However, independent of the substrate type, the uncapped thin MoS₂ films had optical contrasts corresponding to thicknesses of 2–5 MLs, further confirmed by AFM on thermal oxide substrates. Furthermore, the range of PL yield was similar for all four types of sample independent of the substrate and capping type, further indicating that ensembles of films with similar distributions of film thicknesses were measured.

Micro-photoluminescence experiments. Low temperature (10 K) micro-PL was carried out on a large number of thin films in a continuous flow He cryostat. The signal was collected and analyzed using a single spectrometer and a nitrogen-cooled charged-coupled device. The sample was excited with a laser at 532 nm. All PL spectra presented in this work were measured in a range of low powers where no dependence on power of PL lineshape was found.

AFM/UFM experiments. As shown elsewhere³³, the ultrasonic force microscopy (UFM) allows imaging of the near-surface features and subsurface interfaces with superior nanometre scale resolution compared to AFM techniques³⁴. In the sample-UFM modality used in this paper³⁵, the sample in contact with the AFM tip is vibrated at small amplitude (0.5–2 nm) and high frequency (2–10 MHz), much higher than the resonance frequencies of the AFM cantilever. The resulting sample stress produces a reaction, that is modified by the voids, subsurface defects or sample-substrate interfaces, and can be detected as an additional ‘ultrasonic’ force. A unique feature of UFM is that it enables nanometre scale resolution imaging of morphology of subsurface nano-structures and interfaces of solid-state objects. In order to interpret the images of a few layer films presented in Fig. 5, one can note that the bright (dark) colors correspond to higher (lower) sample stiffness.

- Novoselov, K. S. *et al.* Two-dimensional atomic crystals. *PNAS* **102**, 10451–10453 (2005).
- Wang, Q. H., Kalantar-Zadeh, K., Kis, A., Coleman, J. N. & Strano, M. S. Electronics and optoelectronics of two-dimensional transition metal dichalcogenides. *Nature Nanotechnology* **7**, 699–712 (2012).
- Splendiani, A. *et al.* Emerging Photoluminescence in Monolayer MoS₂. *Nano Letters* **10**, 1271–1275 (2010).
- Mak, K., Lee, C., Hone, J., Shan, J. & Heinz, T. Atomically Thin MoS₂: A New Direct-Gap Semiconductor. *Phys. Rev. Lett.* **105**, 136805 (2010).
- Eda, G. *et al.* Photoluminescence from Chemically Exfoliated MoS₂. *Nano Letters* **11**, 5111–5116 (2011).
- Sundaram, R. S. *et al.* Electroluminescence in Single Layer MoS₂. *Nano Letters* **13**, 1416–1421 (2013).
- Radisavljevic, B., Radenovic, a., Brivio, J., Giacometti, V. & Kis, A. Single-layer MoS₂ transistors. *Nature Nanotechnology* **6**, 147–150 (2011).
- Mak, K. F., He, K., Shan, J. & Heinz, T. F. Control of valley polarization in monolayer MoS₂ by optical helicity. *Nature Nanotechnology* **7**, 494–498 (2012).
- Sallen, G. *et al.* Robust optical emission polarization in MoS₂ monolayers through selective valley excitation. *Phys. Rev. B* **86**, 081301(R) (2012).



10. Zeng, H., Dai, J., Yao, W., Xiao, D. & Cui, X. Valley polarization in MoS₂ monolayers by optical pumping. *Nature Nanotechnology* **7**, 490–493 (2012).
11. Cao, T. *et al.* Valley-selective circular dichroism of monolayer molybdenum disulphide. *Nature Communications* **3**, 887 (2012).
12. Xiao, D., Liu, G.-B., Feng, W., Xu, X. & Yao, W. Coupled Spin and Valley Physics in Monolayers of MoS₂ and Other Group-VI Dichalcogenides. *Phys. Rev. Lett.* **108**, 196802 (2012).
13. Jena, D. & Konar, A. Enhancement of Carrier Mobility in Semiconductor Nanostructures by Dielectric Engineering. *Phys. Rev. Lett.* **98**, 136805 (2007).
14. Plechinger, G. *et al.* Low-temperature photoluminescence of oxide-covered single-layer MoS₂. *Phys. Status Solidi RRL* **6**, 126–128 (2012).
15. Yan, R. *et al.* Raman and Photoluminescence Study of Dielectric and Thermal Effects on Atomically Thin MoS₂. *arXiv:1211.4136v1 [cond-mat.mtrl-sci]* (2012).
16. Mak, K. F. *et al.* Tightly bound trions in monolayer MoS₂. *Nature Materials* **11**, 1–5 (2012).
17. Dolui, K., Rungger, I. & Sanvito, S. Origin of the n-type and p-type conductivity of MoS₂ monolayers on a SiO₂ substrate. *Phys. Rev. B* **87**, 165402 (2013).
18. Zhan, Y., Liu, Z., Najmaei, S., Ajayan, P. M. & Lou, J. Large-Area Vapor-Phase Growth and Characterization of MoS₂ Atomic Layers on a SiO₂ Substrate. *Small* **8**, 966–971 (2012).
19. De Wolf, S., Agostinelli, G., Beaucarne, G. & Vitano, P. Influence of stoichiometry of direct plasma-enhanced chemical vapor deposited films and silicon substrate surface roughness on surface passivation. *J. of Appl. Phys.* **97**, 063303 (2005).
20. Boogaard, A., Kovalgin, A. & Wolters, R. Net negative charge in low-temperature SiO₂ gate dielectric layers. *Microelectronic Engineering* **86**, 1707–1710 (2009).
21. Zou, X. & Zhang, J. Study on PECVD SiO₂/Si₃N₄ double-layer electrets with different thicknesses. *Science China Technological Sciences* **54**, 2123–2129 (2011).
22. Peelaers, H. & Van de Walle, C. G. Effects of strain on band structure and effective masses in MoS₂. *Phys. Rev. B* **86**, 241401 (2012).
23. Conley, H. J. *et al.* Bandgap Engineering of Strained Monolayer and Bilayer MoS₂. *arXiv:1305.3880 [cond-mat.mes-hall]* (2013).
24. He, K., Poole, C., Mak, K. F. & Shan, J. Experimental demonstration of continuous electronic structure tuning via strain in atomically thin MoS₂. *arXiv:1305.3673 [cond-mat.mes-hall]* (2013).
25. Castellanos-Gomez, A. *et al.* Local Strain Engineering in Atomically Thin MoS₂. *Nano Letters*; DOI:10.1021/nl402875m (2013).
26. Zhu, C. R. *et al.* Strain tuning of optical emission energy and polarization in monolayer and bilayer MoS₂. *Phys. Rev. B* **88**, 121301(R) (2013).
27. Zhang, X. *et al.* Raman spectroscopy of shear and layer breathing modes in multilayer MoS₂. *Phys. Rev. B* **87**, 115413 (2013).
28. Rice, C. *et al.* Raman-scattering measurements and first-principles calculations of strain-induced phonon shifts in monolayer MoS₂. *Phys. Rev. B* **87**, 081307 (R) (2013).
29. Chakraborty, B. *et al.* Symmetry-dependent phonon renormalization in monolayer MoS₂ transistor. *Phys. Rev. B* **85**, 161403(R) (2012).
30. Buscema, M., Steele, G. A., van der Zant, H. S. J. & Castellanos-Gomez, A. The effect of the substrate on the Raman and photoluminescence emission of single layer MoS₂. *arXiv:1311.3869 [cond-mat.mtrl-sci]* (2013).
31. Scheuschner, N. *et al.* Photoluminescence of freestanding single- and few-layer MoS₂. *arXiv:1311.5824 [cond-mat.mtrl-sci]* (2013).
32. Benameur, M. M. *et al.* Visibility of dichalcogenide nanolayers. *Nanotechnology* **22**, 125706 (2011).
33. Kolosov, O. & Yamanaka, K. Nonlinear Detection of Ultrasonic Vibrations in an Atomic Force Microscope. *Jpn. J. Appl. Phys.* **7** (1993).
34. Yamanaka, K., Ogiso, H. & Kolosov, O. Analysis of Subsurface Imaging and Effect of Contact Elasticity in the Ultrasonic Force Microscope. *Appl. Phys. Lett.* **64**, 178 (1994).
35. McGuigan, A. P. *et al.* Measurement of debonding in cracked nanocomposite films by ultrasonic force microscopy. *Appl. Phys. Lett.* **80**, 1180 (2002).

Acknowledgments

This work has been supported by the Marie Curie ITNs S³NANO and Spin-Optronics, EPSRC Programme grant EP/J007544/1, and EU FP7 GRENADA grant. O. D. P.-Z. thanks CONACYT-Mexico Doctoral Scholarship.

Author contributions

D.S. and S.S. made the samples. D.S., S.S., O.D.P.-Z., F.L., I.I.T. and E.A.C. measured and analyzed optics data. B.J.R. and O.K. measured AFM and UFM. D.S. and A.I.T. wrote the manuscript with input from all co-authors. E.A.C. supervised optical spectroscopy experiments. A.I.T. guided the project.

Additional information

Competing financial interests: The authors declare no competing financial interests.

How to cite this article: Sercombe, D. *et al.* Optical investigation of the natural electron doping in thin MoS₂ films deposited on dielectric substrates. *Sci. Rep.* **3**, 3489; DOI:10.1038/srep03489 (2013).



This work is licensed under a Creative Commons Attribution 3.0 Unported license. To view a copy of this license, visit <http://creativecommons.org/licenses/by/3.0>